

Near-field limits on the role of faint galaxies in cosmic reionization

Michael Boylan-Kolchin,^{1*} James S. Bullock,² and Shea Garrison-Kimmel²

¹*Department of Astronomy and Joint Space-Science Institute, University of Maryland, College Park, MD 20742, USA*

²*Center for Cosmology, Department of Physics and Astronomy, 4129 Reines Hall, University of California, Irvine, CA 92697, USA*

31 October 2018

ABSTRACT

Reionizing the Universe with galaxies appears to require significant star formation in low-mass halos at early times, while local dwarf galaxy counts tell us that star formation has been minimal in small halos around us today. Using simple models and the ELVIS simulation suite, we show that reionization scenarios requiring appreciable star formation in halos with $M_{\text{vir}} \approx 10^8 M_{\odot}$ at $z = 8$ are in serious tension with galaxy counts in the Local Group. This tension originates from the seemingly inescapable conclusion that 30 – 60 halos with $M_{\text{vir}} > 10^8 M_{\odot}$ at $z = 8$ will survive to be distinct *bound* satellites of the Milky Way at $z = 0$. Reionization models requiring star formation in such halos will produce dozens of bound galaxies in the Milky Way’s virial volume today (and 100 – 200 throughout the Local Group), each with $\gtrsim 10^5 M_{\odot}$ of *old* stars ($\gtrsim 13$ Gyr). This exceeds the stellar mass function of classical Milky Way satellites today, even without allowing for the (significant) post-reionization star formation observed in these galaxies. One possible implication of these findings is that star formation became sharply inefficient in halos smaller than $\sim 10^9 M_{\odot}$ at early times, implying that the high- z luminosity function must break at magnitudes brighter than is often assumed (at $M_{\text{UV}} \simeq -14$). Our results suggest that *JWST* (and possibly even *HST* with the Frontier Fields) may realistically detect the faintest galaxies that drive reionization. It remains to be seen how these results can be reconciled with the most sophisticated simulations of early galaxy formation at present, which predict substantial star formation in $M_{\text{vir}} \sim 10^8 M_{\odot}$ halos during the epoch of reionization.

Key words: cosmology: theory – galaxies: dwarf – galaxies: high-redshift

1 INTRODUCTION

Star formation in the low redshift Universe is highly inefficient, both in a galaxy-by-galaxy and in an ensemble-averaged sense. Less than 20% of the cosmic fraction of baryons in a typical Milky Way-mass dark matter halo has been converted into stars by $z = 0$ (Moster et al. 2010; Guo et al. 2010; Behroozi et al. 2013). The conversion efficiency drops to much lower values in smaller halos: at $M_{\text{vir}} = 10^{10} M_{\odot}$, less than 1% of a halo’s baryonic allotment is in the form of stars at the present day. This forms a stark contrast with the situation needed for reionizing the Universe with star-forming galaxies, as current models require high star formation rates in low-mass halos in order to initiate and maintain reionization while also matching the WMAP/Planck optical depth to electron scattering (e.g., Trenti et al. 2010; Kuhlen & Faucher-Giguère 2012; Robertson et al. 2013). Some estimates suggest that galaxies as

faint as $M_{\text{UV}} = -10$ may be required to match the observed optical depth, which, given the high comoving number densities implied, would demand that low-mass halos (with $M_{\text{vir}} \simeq 10^8 M_{\odot}$) are forming stars efficiently at these times (Schultz et al. 2014).

Numerical simulations predict that many halos that were massive enough to form stars efficiently at high redshift have surviving, bound descendants in the region surrounding the Milky Way (MW) today, indicating that there should be a large number of potentially observable remnants of the reionization epoch in the near field. However, the small number of low-mass galaxies in our vicinity strongly constrains the efficiency of star formation at high redshift, not only in mini-halos (Madau et al. 2008), but also in halos that are above the atomic cooling limit of $T_{\text{vir}} \approx 10^4$ K, where cooling can proceed via collisional line excitation of atomic hydrogen rather than relying on the formation of H_2 . In this paper, we place constraints on the efficiency and nature of star formation in low-mass halos during reionization by leveraging the wealth of existing near-field data.

* email: mbk@astro.umd.edu

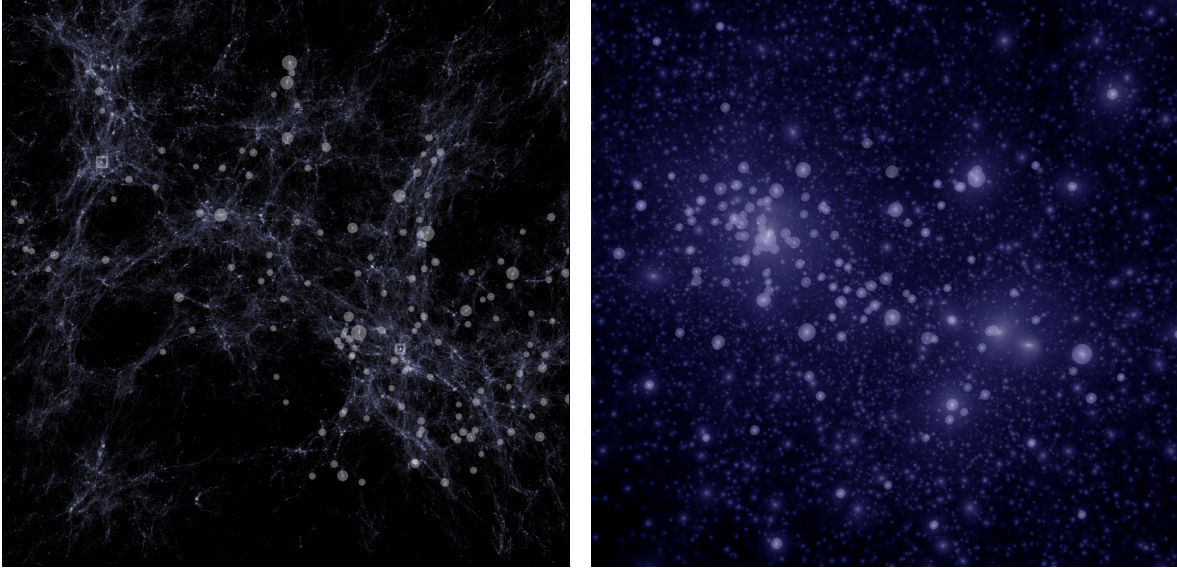


Figure 1. *Left:* Density distribution at $z = 8$ in a 10×10 comoving Mpc region around the progenitor of a Local Group analog. Halos that have $M_{\text{vir}}(z = 8)$ above the atomic cooling limit and that are the main branch progenitor of objects surviving to $z = 0$ are marked with gray circles, while main branch progenitors of the MW/M31 analogs are marked with gray squares. *Right:* Image of the same system at $z = 0$ (1.5×1.5 Mpc). Descendants of the $z = 8$ halos marked in the left panel are shown with gray spheres, sized proportional to their $z = 8$ virial radii. There are approximately 140 identified objects in each image.

2 SIMULATIONS, DATA, AND MODELS

To connect the Local Volume – defined here as a sphere of radius 1.2 Mpc centered on the Local Group barycenter – to the high-redshift Universe, we use the ELVIS suite (Garrison-Kimmel et al. 2014), which is a set of zoom-in simulations of Local Group (LG) analogs embedded in large high-resolution regions. The primary simulations were performed in a WMAP7 cosmology¹ (Komatsu et al. 2011) using particle masses of $1.9 \times 10^5 M_{\odot}$ in the high-resolution regions with a Plummer-equivalent force softening of 141 pc. Halo catalogs in ELVIS are complete to $M_{\text{sub}} = 2 \times 10^7 M_{\odot}$, or equivalently, $V_{\text{max}} = 8 \text{ km s}^{-1}$. The convergence values in terms of “peak” quantities (defined along a halo’s main branch) are $M_{\text{peak}} = 6 \times 10^7 M_{\odot}$ or $V_{\text{peak}} = 12 \text{ km s}^{-1}$. This is sufficient to resolve all halos above the atomic cooling limit of $V_{\text{vir}} \approx 17 \text{ km s}^{-1}$ or $M_{\text{vir}}(z = 8) \approx 10^8 M_{\odot}$. Merger trees are available for all of the ELVIS simulations; in this paper, we use a version of the trees that tracks the most massive progenitor at each snapshot, which is slightly different from what the standard trees provide. Further details about the ELVIS suite can be found in Garrison-Kimmel et al. (2014).

Fig. 1 gives an initial visual impression of the matter distribution around a LG analog, ‘Zeus and Hera’, at $z = 8$ (left) and $z = 0$ (right). Massive ($M_{\text{vir}} > 10^8 M_{\odot}$) objects at $z = 8$ with an identifiable descendant at $z = 0$ are highlighted with gray spheres, sized proportional to $r_{\text{vir}}(z = 8)$ in both images. Only atomic-cooling halos at $z = 8$ that are the most massive progenitors of bound $z = 0$ objects are marked, i.e., there is a one-to-one correspondence between the circled halos in the left panel and those in the right. There are approximately 140 surviving, bound halos in

and around this LG analog that had main-progenitor masses above the atomic cooling limit at $z = 8$ and are therefore good potential sites for early galaxy formation. In subsequent sections, we quantify the number of massive $z = 8$ halos surviving to $z = 0$ in the Local Volume and investigate the resulting implications for reionization scenarios.

Maintaining cosmological reionization with galaxies requires a cosmological star formation rate density (SFRD) that exceeds a critical value of

$$\dot{\rho}_{\text{SFR}} \approx 0.018 M_{\odot} \text{ yr}^{-1} \text{ Mpc}^{-3} \left(\frac{1+z}{8} \right)^3 \frac{C_3}{f_{\text{esc},0.2}} T_4^{-0.845} \quad (1)$$

(Madau et al. 1999; Shull et al. 2012). This critical SFRD depends on the effective clumping factor $C_{\text{H}} \equiv \langle n_{p+}^2 \rangle / \langle n_{p+} \rangle^2$ of ionized hydrogen ($C_3 = C_{\text{H}}/3$) and the escape fraction f_{esc} of ionizing photons from galaxies ($f_{\text{esc},0.2} = f_{\text{esc}}/0.2$), as well as the temperature of the inter-galactic medium, $T_4 \equiv T_{\text{IGM}}/10^4 \text{ K}$. We assume that the star formation rate is a function of halo mass, with

$$\dot{M}_{\star} = \dot{M}_{10} \left(\frac{M_{\text{vir}}}{10^{10} M_{\odot}} \right)^{\beta} \quad (2)$$

for halo masses above a critical value M_c and $\dot{M}_{\star} = 0$ for $M_{\text{vir}} < M_c$. We then have

$$\dot{\rho}_{\text{SFR,sim}} = \dot{M}_{10} \int_{M_c}^{\infty} \left(\frac{M}{10^{10} M_{\odot}} \right)^{\beta} \frac{dn}{dM} dM. \quad (3)$$

For any value of M_c and β , we can determine the required normalization \dot{M}_{10} of the star formation rate to reionize the Universe with galaxies through a comparison with Eqn. 1. Figure 2 shows contours of the required \dot{M}_{10} (in units of $M_{\odot} \text{ yr}^{-1}$) at $z = 8$ in $M_c - \beta$ space, adopting the mass function for dark matter halos given by Sheth & Tormen (1999) [which, we have confirmed, gives a good match to the halo abundance in the simulations of Schultz et al.

¹ Specifically, the cosmological parameters are $\Omega_{\text{m}} = 0.266$, $\Omega_{\Lambda} = 0.734$, $n_s = 0.963$, and $h \equiv H_0/(100 \text{ km s}^{-1} \text{ Mpc}^{-1}) = 0.71$.

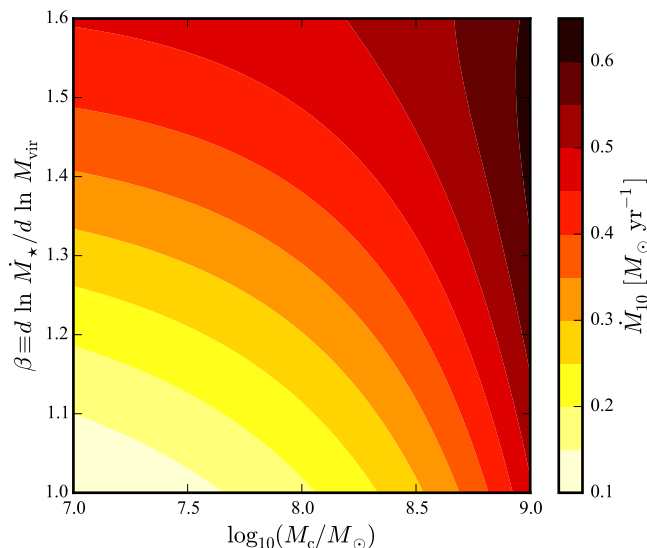


Figure 2. The star formation rate in $10^{10} M_{\odot}$ halos at $z = 8$, $\dot{M}_{10} [M_{\odot} \text{ yr}^{-1}]$, required for reionization as a function of the minimum halo mass for star formation (M_c) and the slope of the $\dot{M}_{\star} - M_{\text{vir}}$ relation, assuming a SFR-halo mass relation given by Eqn. 2. For typical estimates of $\beta \sim 1.35$ and $\dot{M}_{10} \approx 0.4$, star formation in halos down to $M_c \approx 10^8 M_{\odot}$ is required. Steeper $\dot{M}_{\star} - M_{\text{vir}}$ relations (larger values of β) require larger values of \dot{M}_{10} at fixed M_c to achieve reionization.

(2014) and Vogelsberger et al. (2014)]. Finlator et al. (2011) find $\beta \approx 1.35$ and $\dot{M}_{10} = 0.42 M_{\odot} \text{ yr}^{-1}$ at $z = 8$ in their simulations, giving $M_c \approx 1.5 \times 10^8 M_{\odot}$ (which is just at their resolution limit) – i.e., star formation is required in all halos above the atomic cooling limit in order to achieve reionization in these simulations. For steeper values of β in the $\dot{M}_{\star} - M_{\text{vir}}$ relation, higher normalizations \dot{M}_{10} and/or lower cut-off masses M_c are required.

3 CONNECTION TO REDSHIFT ZERO

In order to schematically associate dark matter halo masses with observed UV luminosity functions at $z = 8$, we use abundance matching (Conroy et al. 2006). As in Sec. 2, we use the Sheth-Tormen halo mass function; we take the UV luminosity function measured by Schenker et al. (2013), which is very similar to that of Schmidt et al. (2014) and Bouwens et al. (2014). As the Hubble UDF is only complete for $M_{\text{UV}} \lesssim -17.5$ at $z = 8$, we extrapolate the Schechter (1976) fit of Schenker et al. to lower luminosities.

The result, shown in Fig. 3, can be directly related to our parameter choices in Eqn. 2 and Fig. 2. Assuming $L_{\text{UV}} \propto \dot{M}_{\star} \propto M_{\text{vir}}^{\beta}$, our abundance matching relation gives $\beta \approx 1.4$. The normalization of the mapping from L_{UV} to \dot{M}_{\star} depends on metallicity and the assumed stellar initial mass function (IMF). For the fiducial value of $\mathcal{K}_{\text{FUV}} = 1.15 \times 10^{-28} M_{\odot} \text{ yr}^{-1}$ given in Madau & Dickinson (2014), we obtain

$$\log_{10} \left(\frac{\dot{M}_{\star}}{M_{\odot} \text{ yr}^{-1}} \right) = -0.4 (M_{\text{UV}} + 18.22), \quad (4)$$

which, combined with the relation shown in Fig. 3, gives

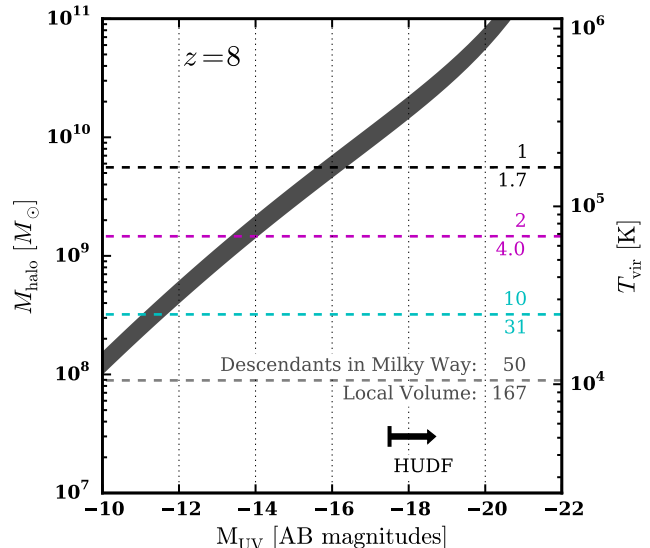


Figure 3. The abundance matching relation between UV luminosity and halo mass at $z = 8$ (thick black curve), which is well-approximated by Eqn. 2 with $\dot{M}_{\star} = 0.33 M_{\odot} \text{ yr}^{-1}$ and $\beta = 1.45$. Also given are counts of identifiable descendant halos at $z = 0$ above a given $z = 8$ mass inside both the simulated MW and Local Volume. There should be approximately 50 surviving remnants in the present-day Milky Way of halos that had masses above the atomic cooling limit, which are predicted to host $M_{\text{UV}}(z = 8) \approx -10$ galaxies. The main progenitor of the Milky Way itself has $M_{\text{UV}} \approx -16$ and is hosted by a halo of $T_{\text{vir}} \approx 1.5 \times 10^5 \text{ K}$ ($M_{\text{vir}} \approx 6 \times 10^9 M_{\odot}$).

$\dot{M}_{10} = 0.33 M_{\odot} \text{ yr}^{-1}$ for the normalization of Eqn. 2. Allowing for variations with age/metallicity gives a range of $0.28 \lesssim \dot{M}_{10}/(M_{\odot} \text{ yr}^{-1}) \lesssim 0.46$, while changing the assumed IMF from Salpeter to Chabrier or Kroupa reduces this normalization by a factor of 1.5–1.6 (Madau & Dickinson 2014); additional effects such as stellar rotation may also reduce the star formation rate at fixed UV luminosity by 30% (Horiuchi et al. 2013). Combined, these effects lead to a factor of $\sim 2 - 3$ uncertainty in the normalization of Eqn. 2, which is not enough to have a qualitative effect on the results discussed in the following sections.

According to Fig. 3, $M_{\text{UV}} = -10$ corresponds to the atomic cooling limit of $M_{\text{vir}} \approx 10^8 M_{\odot}$, while halos with $M_{\text{vir}} \approx 10^9 M_{\odot}$ typically host galaxies with $M_{\text{UV}} = -13$. The faintest $z = 8$ galaxies in the HUDF have $M_{\text{UV}} \approx -17.5$, corresponding to a halo mass of $\approx 10^{10} M_{\odot}$. Figure 3 also indicates, for a variety of $z = 8$ halo masses, the average counts of surviving descendants at $z = 0$ within 300 kpc of a Local Group giant (labeled ‘Milky Way’) or within 1.2 Mpc of the LG barycenter (labeled ‘Local Volume’). The main progenitor of the Milky Way is predicted to have a virial mass of approximately $6 \times 10^9 M_{\odot}$ ($T_{\text{vir}} \approx 1.5 \times 10^5 \text{ K}$) at $z = 8$, corresponding to $M_{\text{UV}} = -16$.

The connection between atomic cooling halos in the epoch of reionization and their local remnants is presented in more detail in Figure 4. The gray curves show cumulative mass functions for the most massive progenitors at $z = 8$ of objects surviving to $z = 0$ within a MW/M31 analog, while the magenta curves show the same quantity within the Local Volume. The upper horizontal axis of the

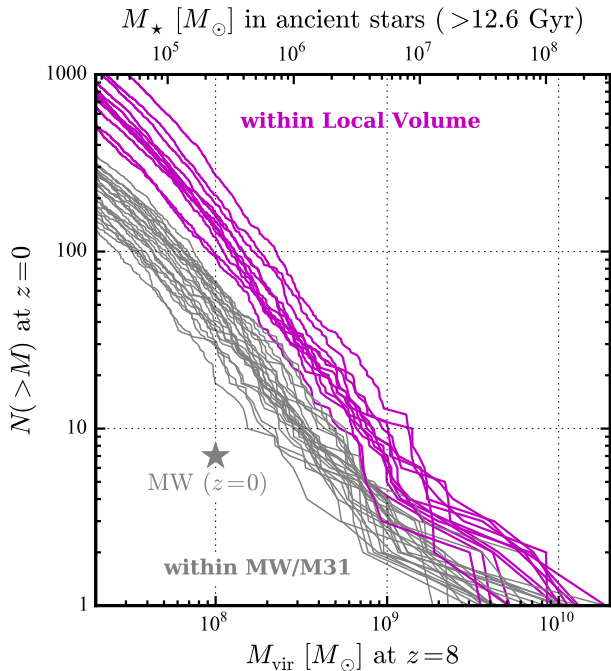


Figure 4. Mass functions at $z = 8$ of the most massive progenitors of dark matter halos within 300 kpc of the MW (gray) or within the Local Volume (magenta) at $z = 0$. The upper horizontal axis gives the mass in old stars (> 12.6 Gyr) associated with each of these bound halos at $z = 0$ (see text for details). This reionization model predicts 20–50 bound galaxies in the MW’s virial volume today that have $> 3 \times 10^5 M_\odot$ of stars that formed before $z = 6$. There are only twelve galaxies with this stellar mass in the Milky Way *at the present day*, almost all of which formed most of their stars after $z = 6$. Only 6–8 MW satellites (gray star) have $M_\star \gtrsim 2 \times 10^5 M_\odot$ in ancient stars (Weisz et al. 2014).

Figure shows the stellar mass in old stars (> 12.6 Gyr) associated with each surviving galaxy assuming a star formation rate at $z = 8$ given by Eqn. 2 with $\dot{M}_{10} = 0.42$ and $\beta = 1.36$, as found in Finlator et al. (2011), and a star formation duration of $\Delta_{t,\text{sf}} = 300$ Myr [the time between $z = 8$ and $z = 6$, or equivalently, $0.3 t_{\text{Hubble}}(z = 8)$]: $M_\star = \Delta_{t,\text{sf}} \dot{M}_{10} (M_{\text{vir}}/10^{10} M_\odot)^\beta$. These stellar masses can be easily scaled for different assumptions about $\Delta_{t,\text{sf}}$. This calculation assumes that there was no star formation prior to $z = 8$; virtually all models predict star formation starting earlier than this in halos at (and below) the atomic cooling limit, which would increase our estimates of the mass contained in ancient stars.

Figure 4 emphasizes the tension between requirements for reionization and the low number of observed satellite galaxies around the MW today. *Within the virial volume of the Milky Way at $z = 0$, there should be ~ 50 distinct remnants of halos that had, at redshift eight, virial masses exceeding the atomic cooling limit; the number grows to ~ 170 when considering the Local Volume.* For models that require star formation in halos at the atomic cooling limit to produce enough ionizing photons through star formation to maintain reionization at these redshifts, a star formation duration of only 100 Myr (rather than the 300 Myr assumed in the Figure) already overproduces the stellar mass function of Local Group galaxies today — 13 galaxies with $M_\star >$

$2 \times 10^5 M_\odot$ in the Milky Way, twice that in M31, and ~ 50 in the Local Volume (e.g., McConnachie 2012) — even though much of the star formation in observed MW satellites happens at significantly later times² (Weisz et al. 2014).

4 DISCUSSION

The competing requirements of efficient star formation in low-mass halos at high redshift to initiate and maintain reionization versus inefficient star formation in low-mass halos (integrated over cosmic time) to match the low number of such halos in and around the Local Group at present strongly constrain reionization scenarios, insofar as the LG is in any way representative. Models that extend to $M_c \approx 10^8 M_\odot$ — approximately $M_{\text{UV}} = -10$, according to our abundance matching relation — will over-produce the number of galaxies having $M_\star > 10^5 M_\odot$ at present (and will do so with only ~ 100 million years of star formation at $z = 8$). To avoid this tension, models must increase the critical mass below which star formation is heavily suppressed to $M_c \sim 10^9 M_\odot$; to still produce enough star formation to reionize the Universe, this increase must be accompanied by an increase in \dot{M}_{10} , an increased ionizing photon output per galaxy, or a shallower SFR-halo mass slope β . Note that relations with $\beta < 1.4$ would necessarily imply that the UV luminosity function must steepen beyond its already steep value of $\alpha \approx -1.9$ (Schenker et al. 2013; Bouwens et al. 2014; Schmidt et al. 2014) at luminosities below the HUDF limit.

4.1 Comparison with previous results

At present, the most sophisticated numerical simulations of reionization-era galaxy formation find high stellar masses ($\gtrsim 10^5 M_\odot$) in halos at or below the atomic cooling limit in the high-redshift universe, supporting the tension discussed this paper. Wise et al. (2012) show that radiation pressure is important in regulating the star formation in a high-resolution simulation of a $z = 8$ dwarf; their simulation produces $M_\star = 4.5 \times 10^5 M_\odot$ in a halo mass of $2.0 \times 10^8 M_\odot$ at $z = 8$. In a follow-up paper, Wise et al. (2014) find that the typical stellar mass of a $10^{8.5} M_\odot$ dark matter halo at $z \sim 8$ is $10^{5.74} M_\odot$, which is very similar to our simple estimate in Figure 4. Simpson et al. (2013) simulate a halo with $M_{\text{vir}}(z = 0) \approx 10^9 M_\odot$ at very high mass and spatial resolution and find that it has formed $10^5 M_\odot$ of stars by $z = 8$, when the halo has a virial mass of $\sim 2 \times 10^7 M_\odot$.

Figure 4 indicates that the Milky Way should contain tens to hundreds of such dwarf satellites today for the Wise et al. and Simpson et al. results, respectively, meaning there should be this number of dwarf galaxies around the MW even without any star formation subsequent to $z \sim 8$. In reality, there are only ~ 12 (30) known satellites of the MW (M31) with $M_\star > 10^5 M_\odot$ at $z = 0$, and all of these have significant star formation after $z = 6$ (Weisz et al. 2014). It appears difficult to avoid the conclusion that typical halos

² We have not considered stellar mass loss, which could, in principle, act to somewhat reduce the stellar mass between $z = 7$ and $z = 0$. However, this effect should not be very large, and we expect will be more than compensated for by additional star formation before $z = 8$ and after $z = 6 - 7$ and by mergers.

of $\sim 10^8 M_\odot$ at $z = 8$ must be forming stars inefficiently, with star formation rates that are considerably lower than the $\dot{M}_* \approx 0.001 - 0.01 M_\odot \text{ yr}^{-1}$ found in many current simulations and models – meaning they should not be major contributors to reionization.

Our results therefore argue for a critical mass closer to $10^9 M_\odot$ rather than $10^8 M_\odot$ in order to avoid over-producing the observed abundance of classical ($L_V > 10^5 L_\odot$) satellites of the Milky Way (and doing so by $z \sim 7$, without any subsequent star formation). A halo mass of $10^9 M_\odot$ corresponds to $M_{UV} \approx -13$ via Figure 3, a value that is at the edge of the allowed values for simultaneous achieving reionization with galaxies and matching the optical depth to electron scattering, according to Robertson et al. (2013).

Our results are complementary to those of Madau et al. (2008), who focused on the star formation in mini-halos $10^6 \lesssim M_{\text{vir}}/M_\odot \lesssim 10^8$ and showed that star formation efficiencies are limited to $\lesssim 10^{-3}$ to avoid over-producing the abundance of ultra-faint dwarfs. Our analysis focuses on somewhat larger mass scales, potentially comparable to progenitors of the classical MW dwarfs, and we find a qualitatively similar result. This concern was also raised by Bovill & Ricotti (2011): they used a hybrid of hydrodynamical and collisionless simulations and also found their models over-produced the number of predicted MW satellites having $L_V > 10^4 L_\odot$. A novel direction of our work is to combine limits derived from abundances of descendants of $z = 8$ halos in the MW with constraints coming from models of reionization. Specifically, we point out that the dwarfs at $z = 0$ might be the same as the ones required for reionization and quantify the resulting implications. The large high-resolution region of each of the ELVIS simulations also enables us to study the distribution of descendants throughout the Local Volume, not just within the virial radius of the Milky Way. In the future, it will be interesting to compare the simulation-based models we have presented here with the detailed extended Press-Schechter (1974) models of, e.g., Muñoz & Loeb (2011) and Salvadori et al. (2014). The interconnection between high-redshift star formation in atomic cooling halos, globular cluster formation, and reionization (Boley et al. 2009), along with the spatial location of the remnants of such halos around the Milky Way today (Gao et al. 2010), is likely to be a fruitful direction for further study.

4.2 Further Implications

Our results provide mass scales at $z = 8$ for expected hosts of MW satellites and for the main progenitor of the Milky Way itself. Approximately fifty distinct progenitors with $z = 8$ masses above $10^8 M_\odot$ survive to end up within 300 kpc of the MW at $z = 0$. *A robust result of our analysis is that the main progenitors of classical MW satellites had masses above the atomic cooling limit at $z = 8$.* If atomic cooling halos play a major role in reionization, the classical MW dwarfs are descendants of these crucial galaxies.

We find that the main progenitor of the Milky Way itself was likely to have a mass of $6 \times 10^9 M_\odot$ at $z = 8$; from the scatter in our simulations, this number could be a factor of three higher or lower. At the high end of this range, Fig. 3 indicates that it would be at the edge of detectability in

the HUDF, and well in the range accessible by the Frontier Fields campaign (Coe et al. 2014).

We note that all of our results only take into account the most massive progenitor of $z = 0$ halos. In reality, many halos at $z = 0$ have multiple progenitors at $z = 8$, meaning we have only provided a lower limit on the stellar mass functions in ancient stars we expect to see in the LG today. If we consider *all* progenitors of everything within the simulated Local Volume at $z = 0$, we find that approximately 50% of progenitor halos with $M_{\text{vir}}(z = 8) > 10^8 M_\odot$ end up merging into the main halo of the Milky Way or M31 while 50% are progenitors of other Local Volume objects at $z = 0$. A further relevant scale of note is the typical peak mass M_{infall} of halos with a given mass at $z = 8$; we find $M_{\text{infall}}/M_{\text{vir}}(z = 8) \approx 5 - 20$ with a median value of ~ 10 (see also fig. 4 of Boylan-Kolchin et al. 2012), indicating that the virial masses of atomic cooling halos grow considerably after $z = 8$. This is also consistent with the aforementioned results of Simpson et al.

Wyithe and Loeb (2013; 2014) have argued for a relatively low duty cycle ($\lesssim 0.1$) of star formation in high-redshift galaxies. The abundance matching results of Figure 3 would need to be modified in this scenario. In particular, since only a fraction of halos would host UV-luminous galaxies in this model, the abundance matching curve would shift to the right such that galaxies of a fixed UV luminosity would be hosted by less massive dark matter halos. If the duty cycle is 10% irrespective of halo mass, then halos with $M_{\text{vir}}(z = 8) = 10^8 M_\odot$ would be expected to host galaxies with $M_{UV} \approx -13$. Although 90% of halos at a given mass would be non-star-forming at any time in this model, the ones that are forming stars do so at a much higher rate than we have assumed above. The product of $\Delta_{t,\text{sf}}$ and \dot{M}_{10} is therefore comparable or even larger than what we have assumed in Sec. 3, once again substantially over-producing the satellite luminosity function of the Milky Way at the present day (see also fig. 6 of Wyithe & Loeb 2013).

Star formation in halos of $M_{\text{vir}} = 10^8 - 10^9 M_\odot$ is expected to be sensitive to the presence of an ionizing background. If the Local Volume was reionized well before $z = 8$, our conclusions would be altered. One interpretation of our results, then, is that Milky Way was indeed reionized early, leading to more negative feedback in low-mass halos destined to end up in the Milky Way and effectively raising M_c in the Milky Way without doing so in the Universe on average. If this is not the case, our results imply that forthcoming deep-field observations with *HST* in the Frontier Fields and with *JWST* may access the smallest galaxies that are important contributors to reionization.

ACKNOWLEDGMENTS

We thank Manoj Kaplinghat and Massimo Ricotti for helpful conversations. Support for this work was provided by NASA through a *Hubble Space Telescope* theory grant (program AR-12836) from the Space Telescope Science Institute (STScI), which is operated by the Association of Universities for Research in Astronomy (AURA), Inc., under NASA contract NAS5-26555. This work was also supported by a matching equipment grant from UC-HiPACC, a multicampus research program funded by the University of California Office of Research.

REFERENCES

- Behroozi, P.S. et al. 2013, *ApJ*, 770, 57
Boley, A.C. et al. 2009, *ApJ*, 706, L192
Bouwens, R.J. et al. 2014, arXiv:1403.4295 [astro-ph]
Bovill, M.S. et al. 2011, *ApJ*, 741, 18
Boylan-Kolchin, M. et al. 2012, *MNRAS*, 422, 1203
Coe, D. et al. 2014, arXiv:1405.0011 [astro-ph]
Conroy, C. et al. 2006, *ApJ*, 647, 201
Finlator, K. et al. 2011, *ApJ*, 743, 169
Gao, L. et al. 2010, *MNRAS*, 403, 1283
Garrison-Kimmel, S. et al. 2014, *MNRAS*, 438, 2578
Guo, Q. et al. 2010, *MNRAS*, 404, 1111
Horiuchi, S. et al. 2013, *ApJ*, 769, 113
Komatsu, E. et al. 2011, *ApJS*, 192, 18
Kuhlen, M. et al. 2012, *MNRAS*, 423, 862
Madau, P. et al. 2014, arXiv:1403.0007 [astro-ph]
—. 1999, *ApJ*, 514, 648
—. 2008, *ApJ*, 689, L41
McConnachie, A.W. 2012, *AJ*, 144, 4
Moster, B.P. et al. 2010, *ApJ*, 710, 903
Muñoz, J.A. et al. 2011, *ApJ*, 729, 99
Press, W.H. et al. 1974, *ApJ*, 187, 425
Robertson, B.E. et al. 2013, *ApJ*, 768, 71
Salvadori, S. et al. 2014, *MNRAS*, 437, L26
Schechter, P. 1976, *ApJ*, 203, 297
Schenker, M.A. et al. 2013, *ApJ*, 768, 196
Schmidt, K.B. et al. 2014, *ApJ*, 786, 57
Schultz, C. et al. 2014, arXiv:1401.3769 [astro-ph]
Sheth, R.K. et al. 1999, *MNRAS*, 308, 119
Shull, J.M. et al. 2012, *ApJ*, 747, 100
Simpson, C.M. et al. 2013, *MNRAS*, 432, 1989
Trenti, M. et al. 2010, *ApJ*, 714, L202
Vogelsberger, M. et al. 2014, *Nature*, (in press)
Weisz, D.R. et al. 2014, arXiv:1404.7144 [astro-ph]
Wise, J.H. et al. 2012, *MNRAS*, 427, 311
—. 2014, arXiv:1403.6123 [astro-ph]
Wyithe, J.S.B. et al. 2013, *MNRAS*, 428, 2741
—. 2014, *MNRAS*, 439, 1326